Supplementary Information

Isomerization Initiated by Photoinduced Ligand Dissociation in Ru(II) Complexes with the Ligand 2-*p*-tolylpyridinecarboxaldimine

Bryan A. Albani,[§] Christopher B. Durr,[§] Bruno Peña,[†] Kim R. Dunbar,[†,*] Claudia Turro[§,*]

[§]*Department of Chemistry and Biochemistry, The Ohio State University, Columbus, OH*
[†]*Department of Chemistry, Texas A&M University, College Station, TX*

Table S1. Crystallographic data for the isolated isomers with the formula $[Ru(PTPI)_2(CH_3CN)_2][PF_6]_2$.

Compound	**α**	**ε**	**δ**	**γ**
Chemical formula	$C_{30}H_{30}F_{12}N_6P_2Ru$	$C_{30}H_{30}F_{12}N_6P_2Ru$	$C_{34}H_{36}F_{12}N_8P_2Ru$	$C_{30}H_{30}F_{12}N_6P_2Ru$
Formula weight	865.61	865.61	947.72	865.61
Temp (K)	152(2)	152(2)	150(2)	150(2)
Space group	Monoclinic, $P2_1/n$	Triclinic, P-1	Triclinic, P-1	Monoclinic C2/*c*
a (Å)	10.2344(2)	10.9107(3)	7.9218(1)	17.9182(4)
b (Å)	20.3040(4)	15.4227(4)	11.0249(1)	14.9211(3)
c (Å)	17.4171(3)	23.2585(6)	11.9521(1)	13.9631(2)
α (°)		103.492(1)	88.284(1)	
β (°)	99.920(1)	102.447(1)	73.575(1)	110.621(1)
γ (°)		98.567(1)	82.065(1)	
V (Å^3)	3565.15(12)	3633.56(17)	991.630(18)	3493.98(12)
Z	4	4	1	4
D_{calcd} (Mg/m^3)	1.613	1.582	1.587	1.646
Crystal size (mm)	0.35 X 0.25 X 0.25	0.38 X 0.38 X 0.12	0.31 X 0.31 X 0.23	0.31 X 0.15 X 0.12
Theta range for data collection (°)	1.554 to 27.484	1.389 to 27.562	1.776 to 27.471	1.827 to 27.466
μ,(Mo, Kα) (mm^{-1})	0.624	0.612	0.570	0.636
Reflections collected	60341	88055	27254	31630
Unique reflections	8170 [R(int)= 0.038]	16697 [R(int)=0.050]	4532 [R(int)=0.028]	4003 [R(int)=0.029]
Data Completeness to [θ]	99.7% [25.242]	100.0% [25.242]	99.9% [25.242]	99.9% [25.242]
Data/restraints/parameters	8170 / 15 / 497	16697 / 0 / 927	4532 / 0 / 262	4003 / 0 / 233
R1[a] (%) (all data)	4.40 (6.40)	5.17 (8.11)	2.91 (3.44)	2.73 (3.55)
wR2[b] (%)(all data)	11.12 (12.19)	14.24 (15.46)	8.20 (9.67)	7.14 (8.48)
Goodness-of-fit on F^2	1.027	1.081	1.197	1.192
Largest diff. peak and hole (e Å^{-3})	0.966 and -0.666	1.055 and -0.782	0.479 and -0.767	0.839 and -0.434

Table S2. Crystallographic data for the complexes $[Ru(bpy)(PTPI)(CH_3CN)_2][PF_6]_2$ and $[Ru(bpy)(pap)(CH_3CN)_2][PF_6]_2$.

Compound	**1**	**2**
Chemical formula	$C_{27}H_{26}F_{12}N_6P_2Ru$	$C_{25}H_{23}F_{12}N_7P_2Ru$
Formula weight	825.55	812.51
Temp (K)	150(2)	150(2)
Space group	Monoclinic, $P2_1/n$	Triclinic, P-1
a (Å)	14.0071(1)	10.4476(5)
b (Å)	14.1691(2)	11.4883(6)
c (Å)	15.9424(2)	13.8038(8)
α (^{o})		89.276(2)
β (^{o})	92.672(1)	70.185(2)
γ (^{o})		72.949(3)
V (Å^3)	3160.62(6)	1483.24(14)
Z	4	2
D_{calcd} (Mg/m^3)	1.735	1.819
Crystal size (mm)	0.19 X 0.19 X 0.12	0.35 X 0.15 X 0.12
Theta range for data collection (^{o})	1.892 to 27.485	1.389 to 25.012
μ,(Mo, Kα) (mm^{-1})	0.699	0.744
Reflections collected	60560	32880
Unique reflections	7249 [R(int)= 0.044]	5223 [R(int)=0.065]
Data Completeness to [θ]	100.0% [25.242]	99.6% [25.000]
Data/restraints/parameters	7249 / 0 / 436	5223 / 0 / 426
R1^a (%) (all data)	3.88 (5.92)	4.53 (6.50)
wR2^b (%)(all data)	10.07 (12.15)	10.91 (11.83)
Goodness-of-fit on F^2	1.102	1.085
Largest diff. peak and hole (e Å^{-3})	1.151 and -0.937	0.956 and -0.471

^{a}R1 = Σ | $|F_o|-|F_c|$ | / Σ $|F_o|$ x 100

^{b}wR2 = [Σ w ($F_o^2-F_c^2$)^2 / Σ (w $|F_o|^2)^2$]$^{1/2}$ x 100

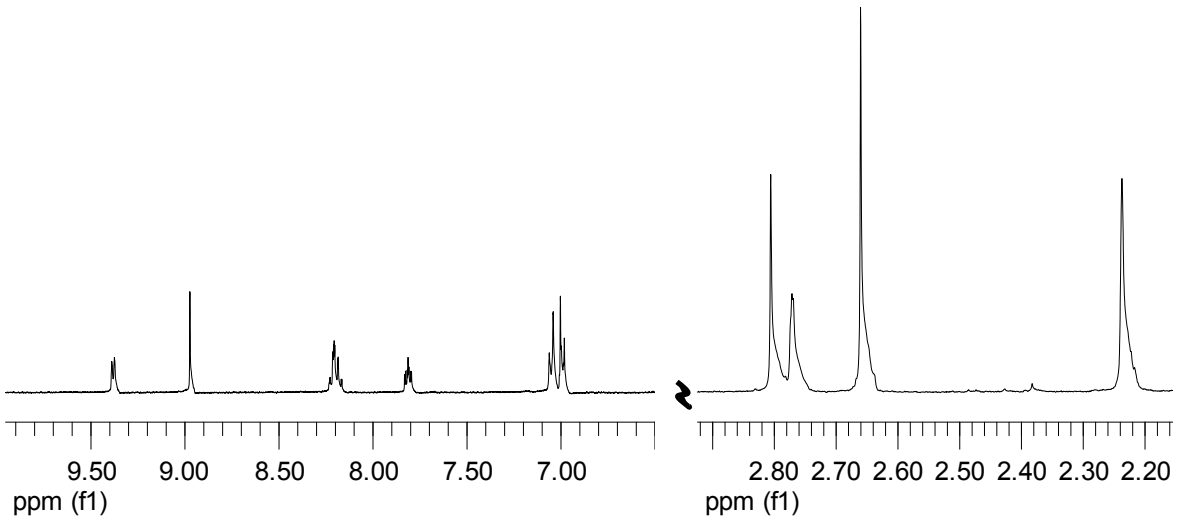

Fig. S1. ^{1}H NMR spectrum of **α**-$[Ru(PTPI)_2(CH_3CN)_2]^{2+}$ in $(CD_3)_2CO$; the resonances at ~2.76 ppm and 2.81 ppm correspond to residual water.

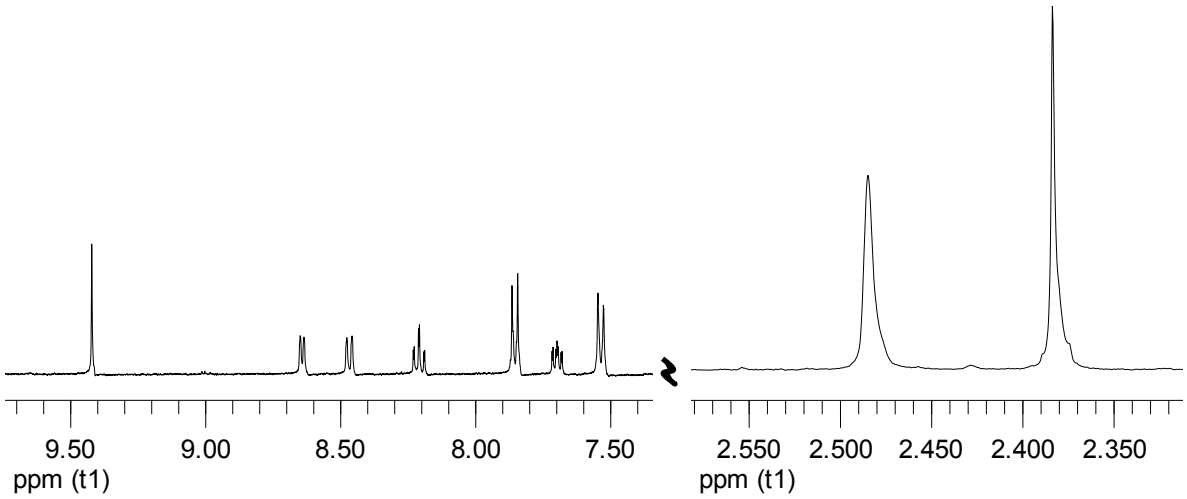

Fig. S2. ^{1}H NMR spectrum of **ε**-$[Ru(PTPI)_2(CH_3CN)_2]^{2+}$ in $(CD_3)_2CO$.

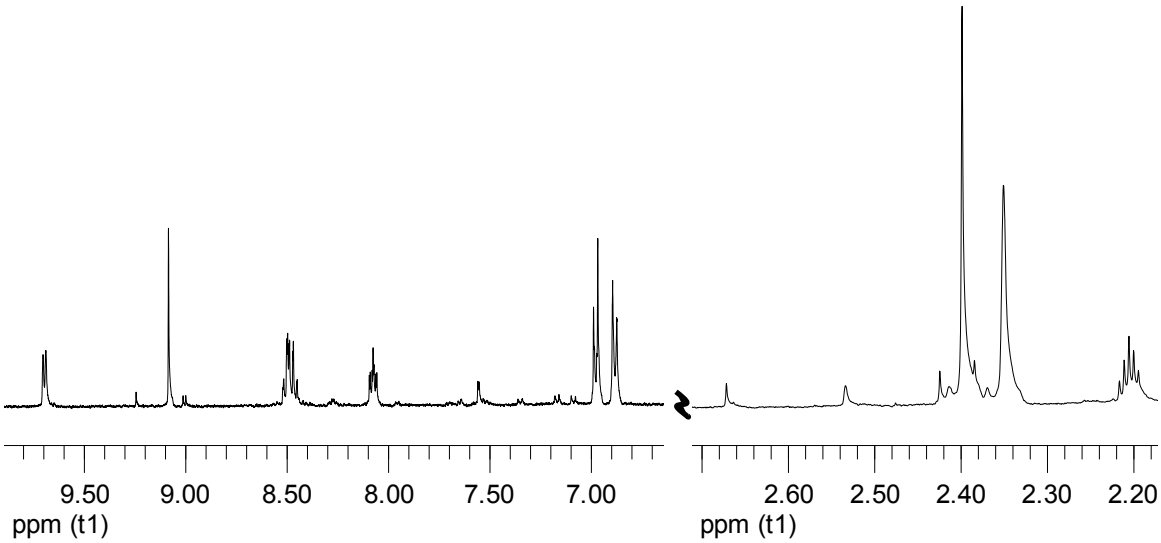

Fig. S3. ^{1}H NMR spectrum of **γ**-$[Ru(PTPI)_2(CH_3CN)_2]^{2+}$ in $(CD_3)_2CO$. Trace amounts of the **δ**-$[Ru(PTPI)_2(CH_3CN)_2]^{2+}$ isomer are present.

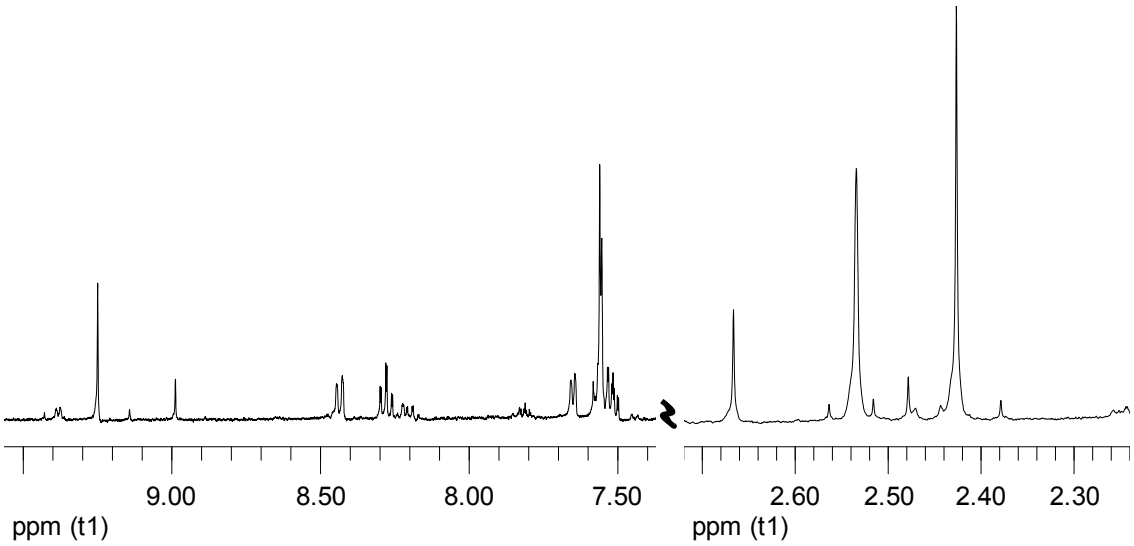

Fig. S4. ^{1}H NMR spectrum of **δ**-$[Ru(PTPI)_2(CH_3CN)_2]^{2+}$ in $(CD_3)_2CO$. Trace amounts of the **γ**-$[Ru(PTPI)_2(CH_3CN)_2]^{2+}$ isomer are present.

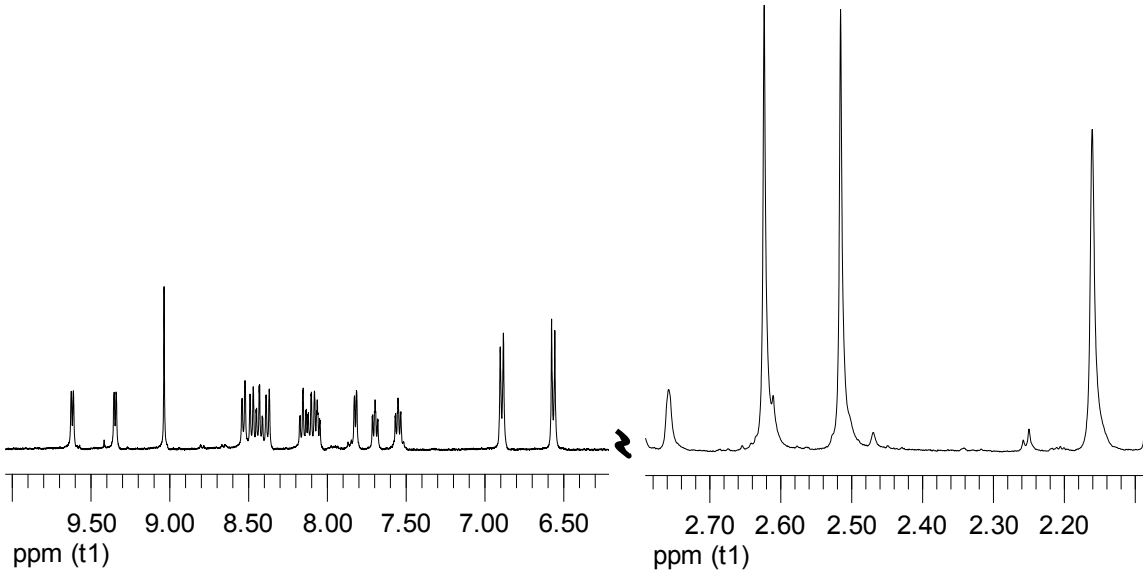

Fig. S5. ^{1}H NMR spectrum of **1** in $(CD_3)_2CO$.

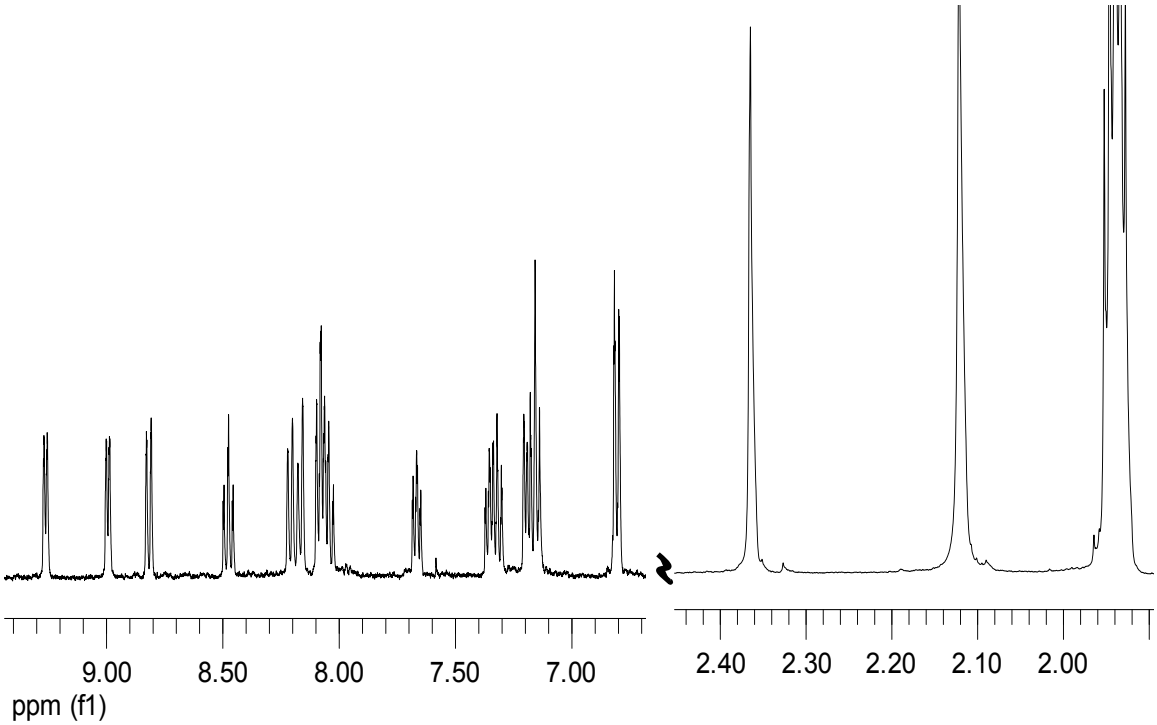

Fig. S6. ^{1}H NMR spectrum of **2** in (CD_3CN). The resonance at 2.13 ppm corresponds to residual water.

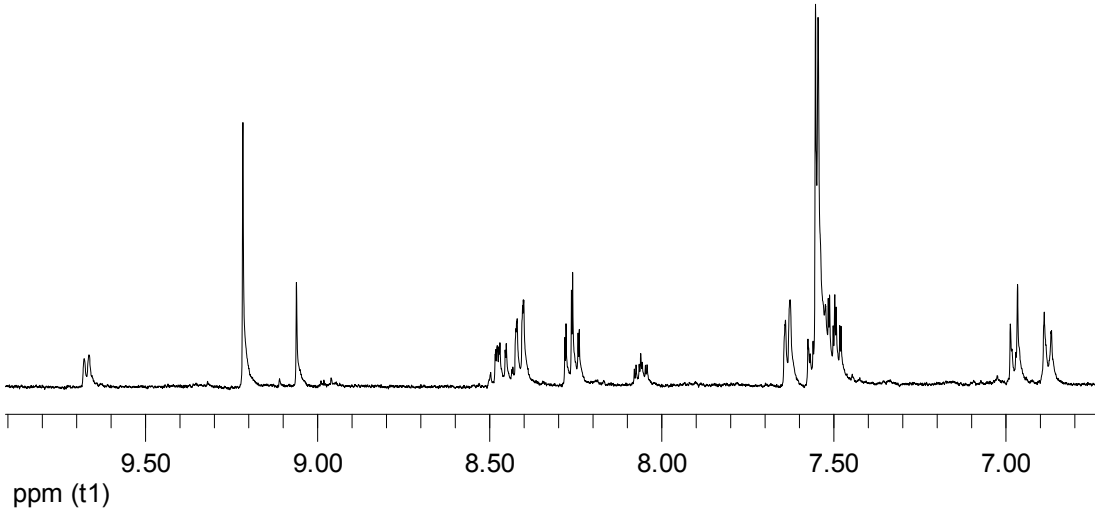

Fig. S7. ^{1}H NMR spectrum of the aromatic region of the initial product containing the mixture of the **δ**-$[Ru(PTPI)_2(CH_3CN)_2]^{2+}$ and **γ**-$[Ru(PTPI)_2(CH_3CN)_2]^{2+}$ isomers in $(CD_3)_2CO$ before recrystallization and separation.

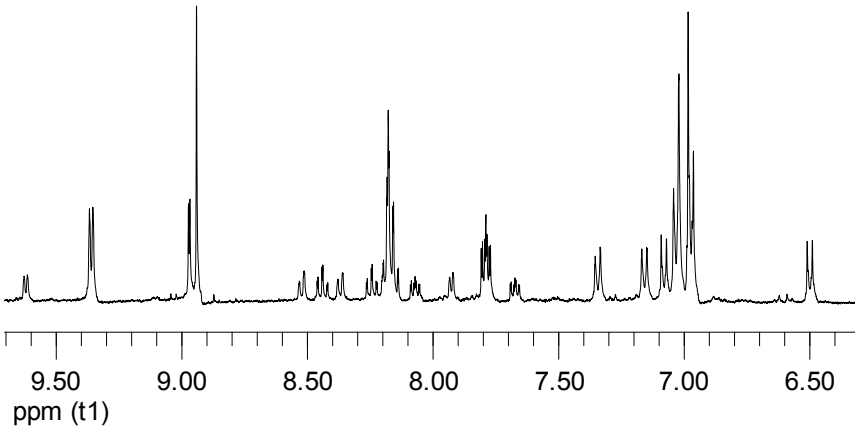

Fig. S8. ^{1}H NMR spectrum of the aromatic region of the initial product containing the mixture of the **α**-$[Ru(PTPI)_2(CH_3CN)_2]^{2+}$ and **β**-$[Ru(PTPI)_2(CH_3CN)_2]^{2+}$ isomers in $(CD_3)_2CO$ before recrystallization and separation of the **α**-$[Ru(PTPI)_2(CH_3CN)_2]^{2+}$ isomer.

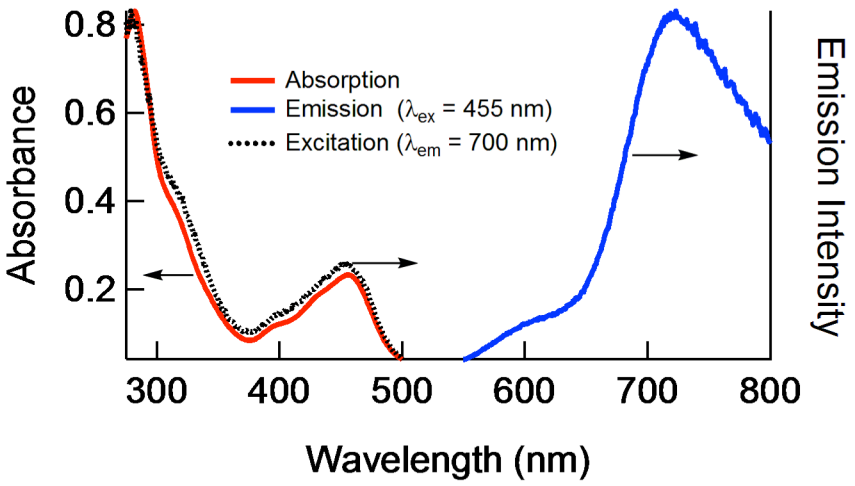

Fig. S9. Emission, absorption, and excitation spectrum of **1** in CH_3CN at room temperature.

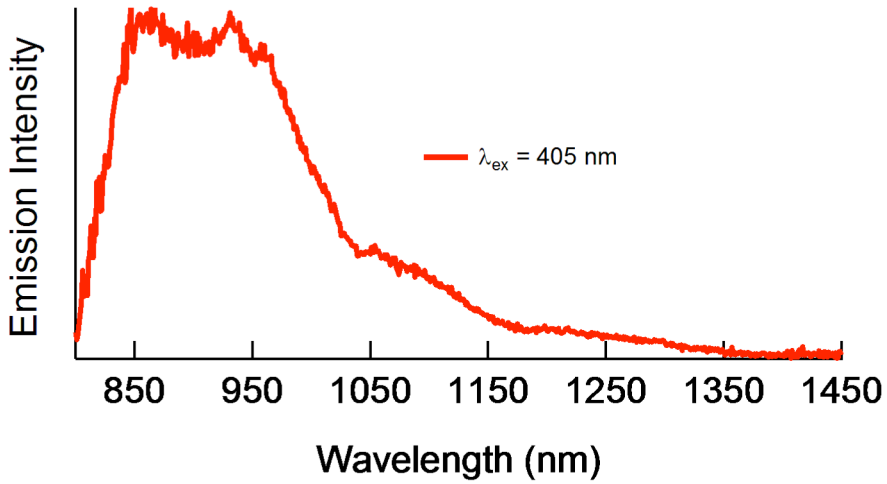

Fig. S10. Emission spectrum of **2** in CH_3CN at 77 K.

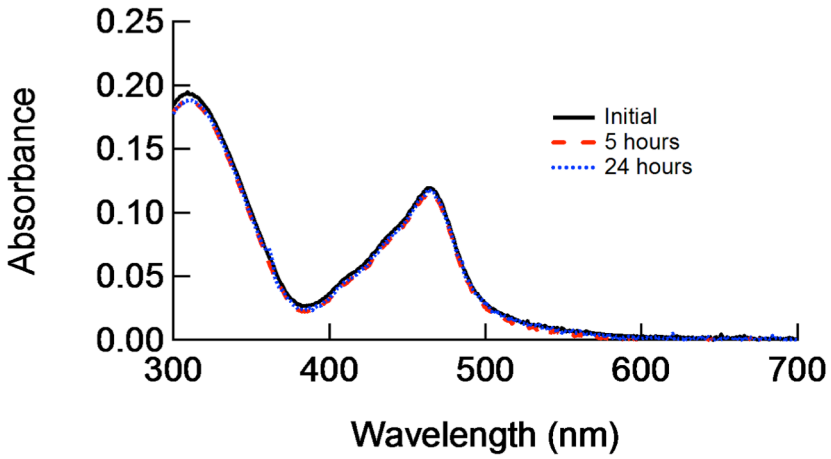

Fig. S11. Thermal stability of the α-$[Ru(PTPI)_2(CH_3CN)_2]^{2+}$ isomer in H_2O.

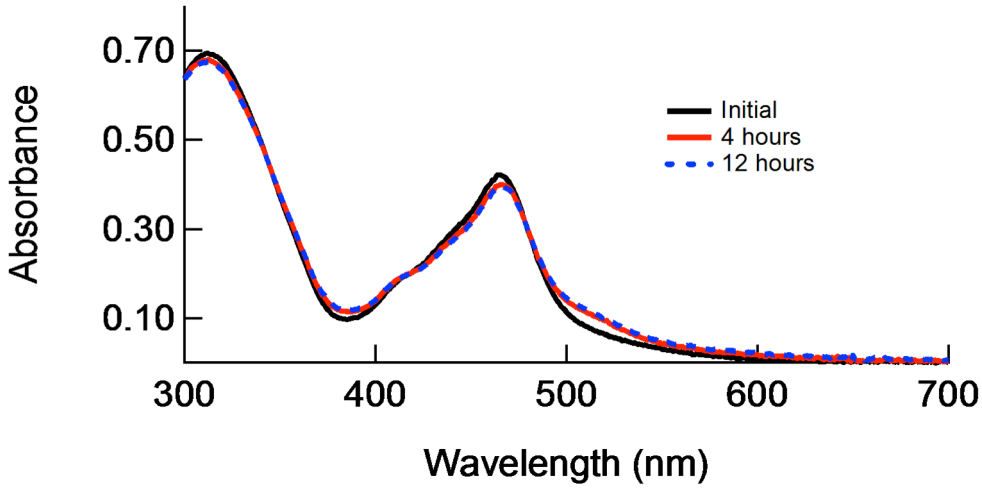

Fig. S12. Thermal stability of the α- $[Ru(PTPI)_2(CH_3CN)_2]^{2+}$ isomer in CH_3CN.

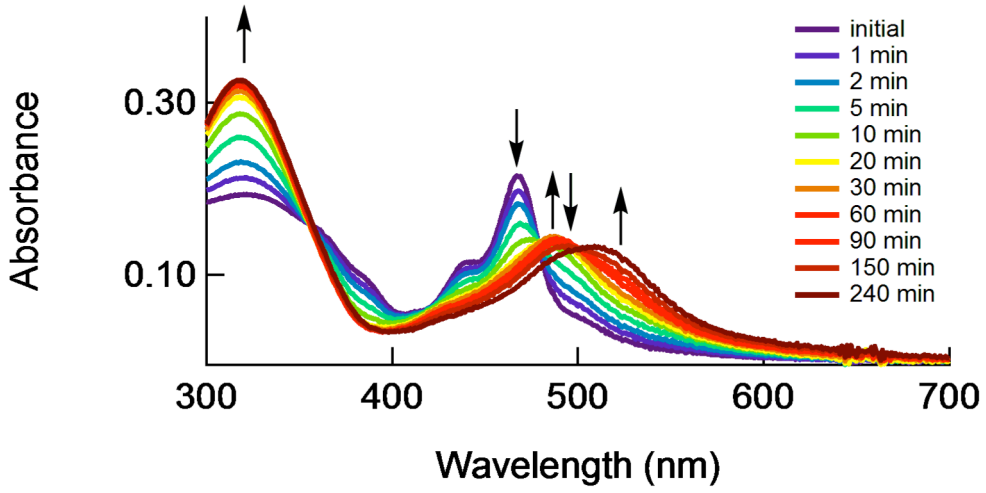

Fig. S13. Changes to the electronic absorption spectrum of **γ**-$[Ru(PTPI)_2(CH_3CN)_2]^{2+}$ in H_2O upon irradiation ($\lambda_{irr} \geq 495$ nm).

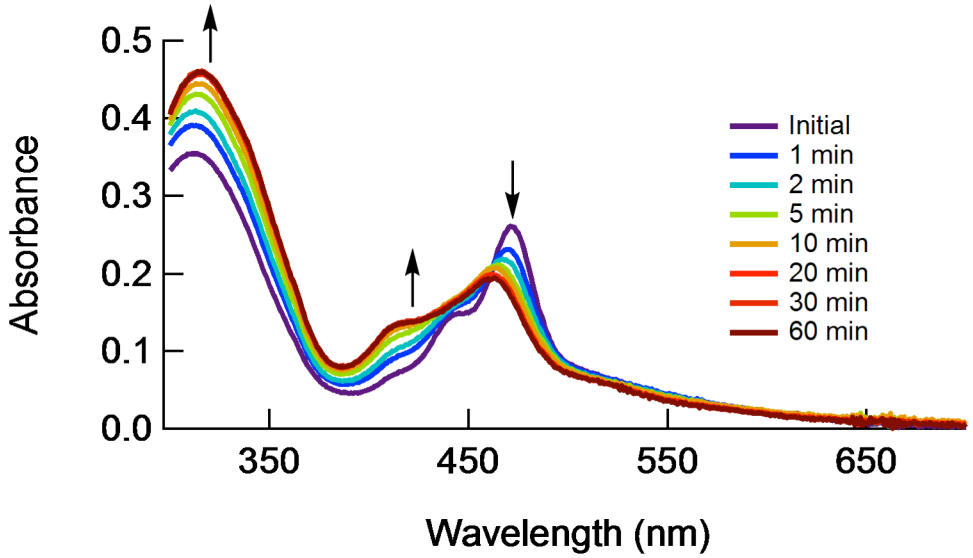

Fig. S14. Changes to the electronic absorption spectrum of **δ**-$[Ru(PTPI)_2(CH_3CN)_2]^{2+}$ in CH_3CN upon irradiation ($\lambda_{irr} \geq 495$ nm).

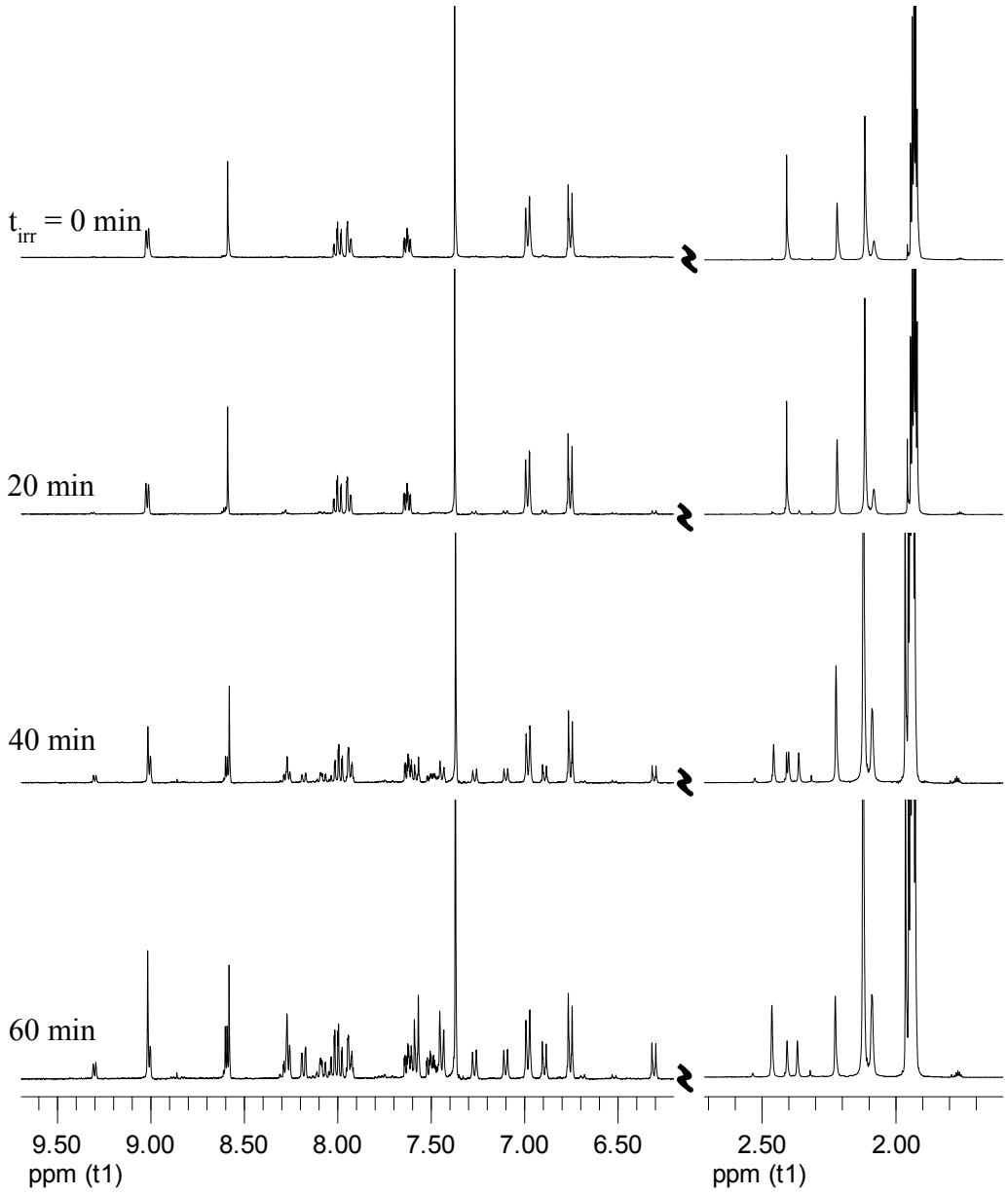

Figure S15. Photolysis of **α**-$[Ru(PTPI)_2(CH_3CN)_2]^{2+}$ monitored by ^1H NMR spectroscopy in CD_3CN $\lambda_{irr} \geq 495$ nm at 0, 20, 40, and 60 minutes. The singlet at 7.35 ppm corresponds to the benzene internal standard, the resonance at 2.45 ppm corresponds to bound CH_3CN and the resonance growing in at 1.96 ppm corresponds to free CH_3CN.

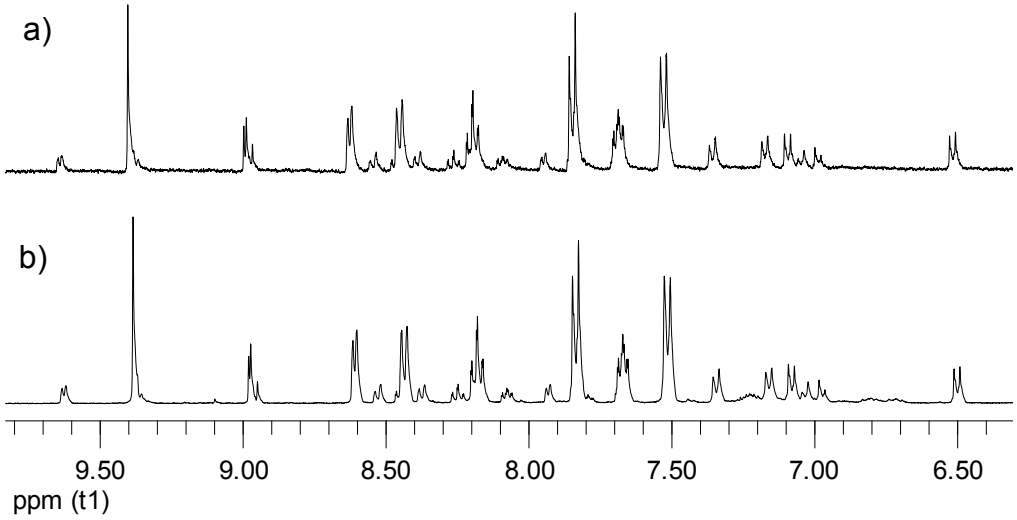

Figure S16. ^{1}H NMR spectra in $(CD_3)_2CO$ of the aromatic region resulting from photolysis ($\lambda_{irr} \geq 420$ in CH_3CN for 4 hours) of a) **α**-$[Ru(PTPI)_2(CH_3CN)_2]^{2+}$ and b) *trans*-$[Ru(PTPI)_2(CH_3CN)_2]^{2+}$ isomers.

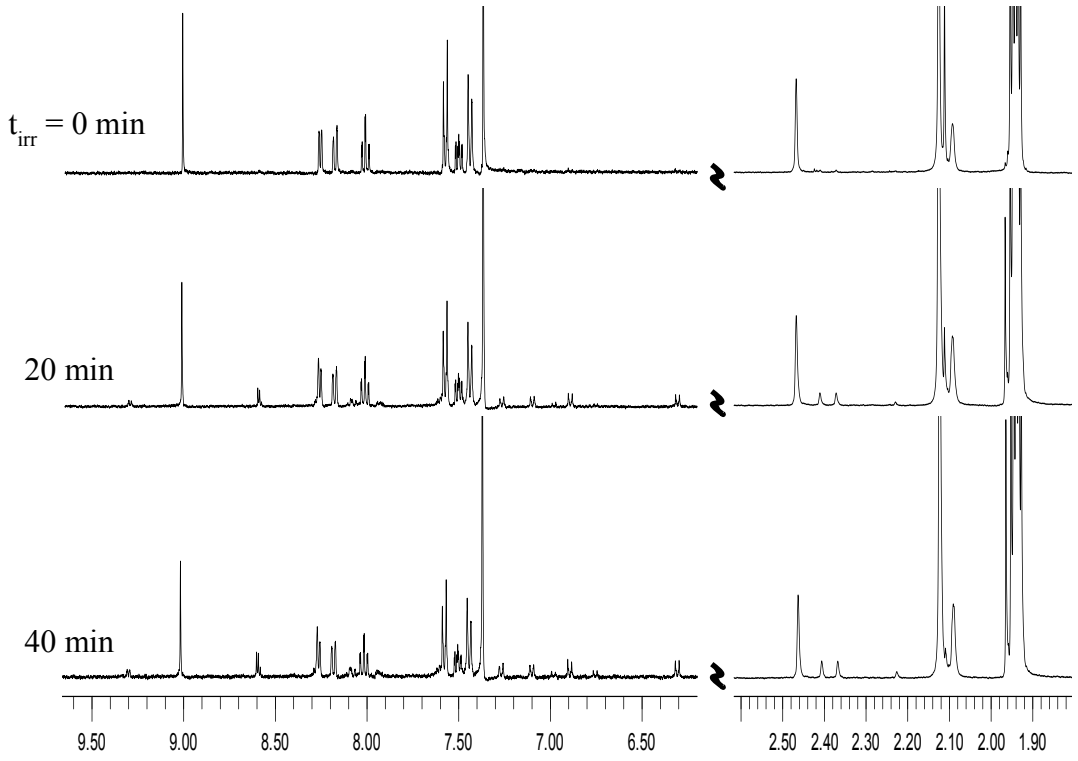

Figure S17. Photolysis of **ε**-$[Ru(PTPI)_2(CH_3CN)_2]^{2+}$ monitored by ^{1}H NMR spectroscopy in CD_3CN $\lambda_{irr} \geq 495$ nm at 0, 20, and 40 minutes. The singlet at 7.35 ppm corresponds to the benzene internal standard, the resonance at 2.10 ppm corresponds to bound CH_3CN, and the resonance growing in at 1.96 ppm corresponds to free CH_3CN.

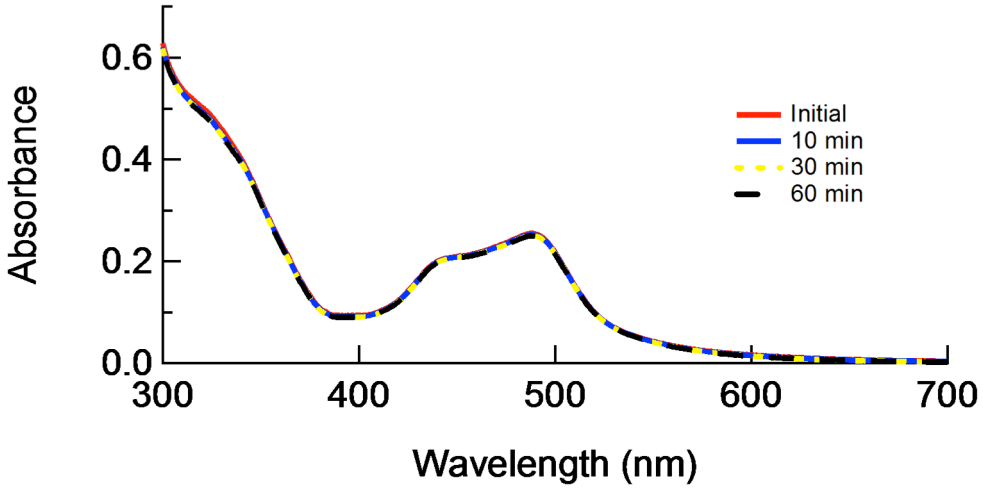

Fig. S18. Stability of **3** in CH_3CN when irradiated with ≥ 420 nm light.

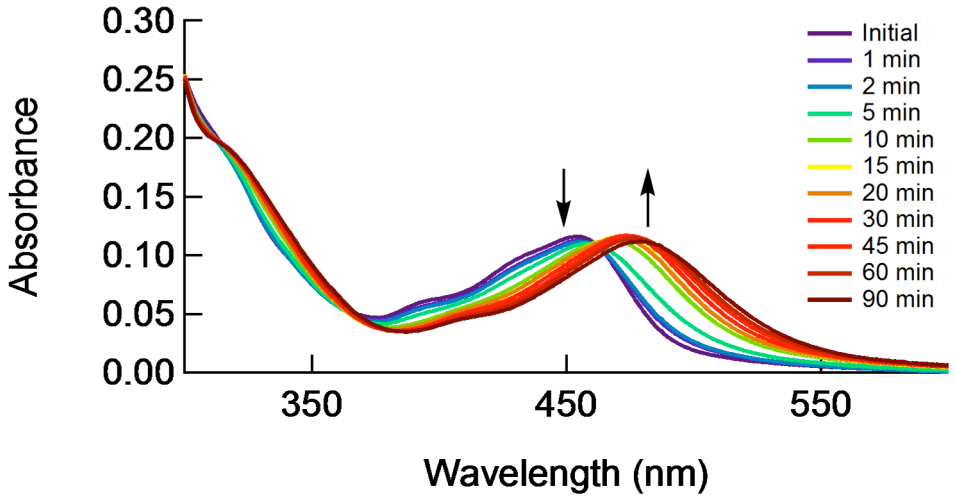

Fig. S19. Changes to the electronic absorption spectrum of **1** in H_2O upon irradiation ($\lambda_{irr} \geq 420$ nm).

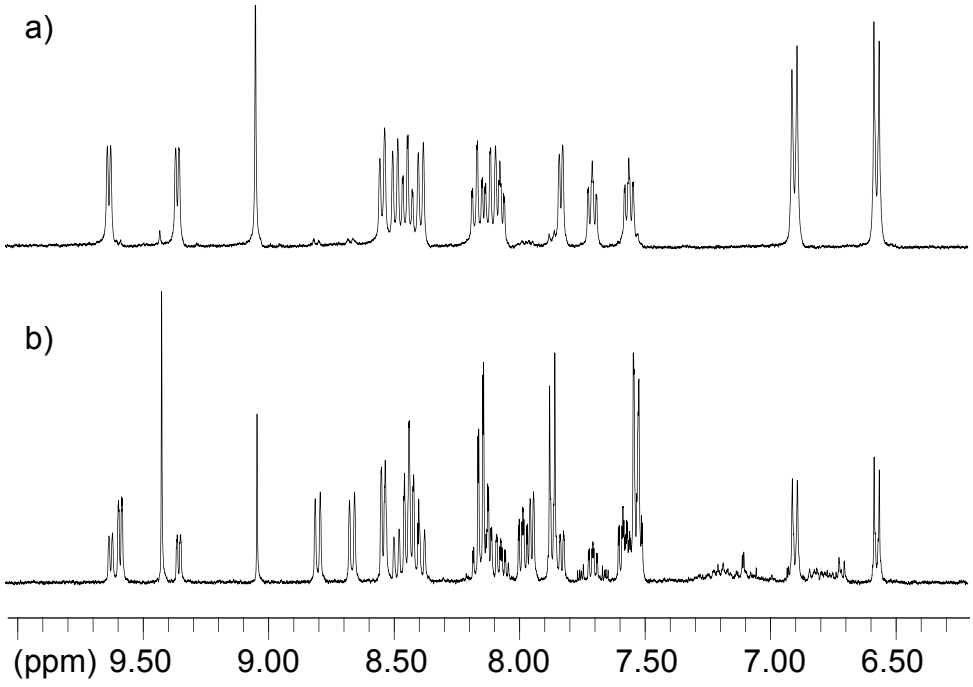

Fig. S20. ^{1}H NMR spectra in $(CD_3)_2CO$ of the aromatic region of **1** a) before and b) after photolysis in CH_3CN ($\lambda_{irr} \geq 420$, 15 hours).

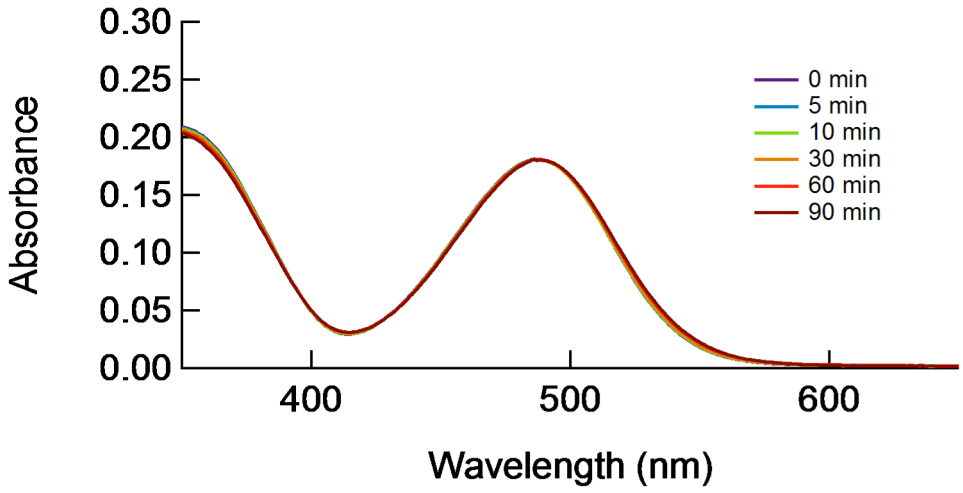

Fig. S21. Changes to the electronic absorption spectrum of **2** in H_2O upon irradiation ($\lambda_{irr} \geq 420$ nm).

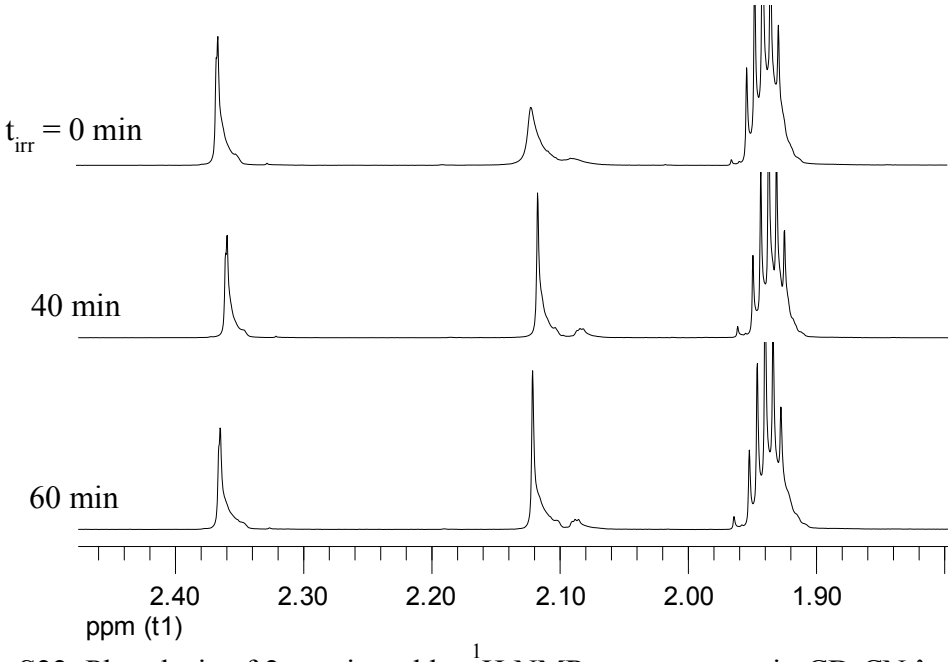

Figure S22. Photolysis of **2** monitored by ^{1}H NMR spectroscopy in CD_3CN $\lambda_{irr} \geq 355$ nm at 0, 40, and 60 minutes. The singlet at 2.36 ppm corresponds to bound CH_3CN and the resonance growing in at 1.96 ppm corresponds to free CH_3CN. The resonance at 2.12 corresponds to residual water.